Biosensors and Bioelectronics 78 (2016) 464–470

Contents lists available at ScienceDirect

Biosensors and Bioelectronics

journal homepage: www.elsevier.com/locate/bios

Ultraspecific electrochemical DNA biosensor by coupling spontaneous cascade DNA branch migration and dual-signaling sensing strategy

Ting Wang [a,1], Lili Zhou [a,1], Shulian Bai [a], Zhang Zhang [a], Junlong Li [a], Xiaoying Jing [b], Guoming Xie [a,*]

[a] Key Laboratory of Laboratory Medical Diagnostics, Ministry of Education, Department of Laboratory Medicine, Chongqing Medical University, No. 1 Yi Xue Yuan Road, Chongqing 400016, PR China
[b] Department of Laboratory Medicine, Affiliated Wuxi People's Hospital of Nanjing Medical University, Wuxi 214023, PR China

ARTICLE INFO

Article history:
Received 25 September 2015
Received in revised form
21 November 2015
Accepted 23 November 2015
Available online 2 December 2015

Keywords:
Spontaneous cascade DNA branch migration
Dual-signaling sensing strategy
Strand displacement reaction
"Signal-on/off" sensing system
Electrochemical biosensor

ABSTRACT

Using spontaneous cascade DNA branch migration and dual-signaling sensing strategy, we developed a novel universal electrochemical biosensor for the highly specific and sensitive detection of nucleic acids. A target strand (Ts) competitively hybridized with a ferrocene (Fc)-labeled signal probe (Fc-S1), which was blocked by a protector strand (Ps), after strand displacement to form the Ts/Fc-S1 duplex. A methylene blue (MB)-modified signal probe (MB-S2) was immobilized on the Au electrode surface by hybridizing with a thiolated capture probe (Cp). Then, the obtained reactants (Ts/Fc-S1 and MB-S2/Cp) suffered spontaneous DNA branch migration and produced two hybridization products (Fc-S1/Cp and MB-S2/Ts). These reactions led to the dissociation of MB molecules and the collection of Fc molecules. The detection mechanism of this DNA biosensor involved distance variation between the redox tags and the Au electrode, which was associated with target-induced cascade DNA branch migration. Moreover, we rationally designed the cascade DNA branch migration to occur spontaneously with $\Delta G^{\circ} \approx 0$, at which slight thermodynamic changes caused by base mismatch exerted a disproportionately large effect on the hybridization yield. This "signal-on/off" sensing system exhibited a remarkable analytical performance and an ultrahigh discrimination capability even against a single-base mismatch. The maximum discrimination factor (DF) of base mutations or alterations can reach 17.9. Therefore, our electrochemical biosensor might hold a great potential for further applications in biomedical research and early clinical diagnosis.

1. Introduction

Nucleic acids are essential biomolecules that encode and regulate the expression of genetic information within living organisms (Collins et al., 2003; Sauna and Kimchi-Sarfaty, 2011). In general, small changes in nucleic acid sequences can lead to significant biological and biomedical implications, such as human diseases, population genetics, and bacterial drug resistance (Chen et al., 2011; Ito et al., 2007). Therefore, the highly selective and sensitive detection of specific nucleic acids is a crucial research goal with an immense potential for biomedical applications. However, the specificity of nucleic acid hybridization, which was simply based on Watson–Crick base-pairing has been challenged except near the melting temperature. High-temperature or chemical denaturation is often used to improve hybridization specificity (Zhang et al., 2012). Nevertheless, the operation near the melting temperature or under chemically denaturing conditions is not always feasible. Hence, new and simple methods for the specific and convenient determination of nucleic acids must be developed.

To date, various methods have been rationally used to generate a high specificity to the target molecule; these methods include strand displacement (Li et al., 2011; Zhang and Winfree, 2010; Zhu et al., 2013), chemically modified probes (Agarwal et al., 2013; Gomez et al., 2014), cooperative hybridization (Chen et al., 2015; Ren et al., 2015; Zhang, 2010), hairpins (Farjami et al., 2011; Li et al., 2014), and other structural elements. Among these devices, strand displacement reaction, in which the invading strand displaces the protector in binding to the substrate with partial complementary to both, was a powerful mechanism that improves the specificity of nucleic acid hybridization (Genot et al., 2011; Qian et al., 2011;

* Corresponding author.
E-mail addresses: guomingxie@cqmu.edu.cn, 504524429@qq.com (G. Xie).
[1] The authors contributed equally to this work and should be considered as co-first authors.

http://dx.doi.org/10.1016/j.bios.2015.11.071
0956-5663/

Wang et al., 2014; Zhang and Seelig, 2011). Moreover, Holliday junction, which primarily relies on double-stranded toehold exchange and spontaneous DNA branch migration, has been recently known to be a mismatch-sensitive recognition structure (Krainer et al., 2015; Panyutin and Hsieh, 1993). Double-stranded probes were designed to hybridize spontaneously with a double-stranded target DNA that proceeds at approximate thermodynamic equilibrium ($\Delta G^\circ \approx 0$) (Chen et al., 2013). Meanwhile, the binding affinity is low when base mutations or alterations are present in the target molecule by taking advantage of small energetic differences near $\Delta G^\circ \approx 0$ can result in strong differences in the hybridization yield (Wang and Zhang, 2015). Thus, the device whose operation is based on DNA strand displacement and Holliday junction can meet the requirement of specificity in nucleic acids analysis.

Electrochemical methods were one of the most promising approaches for nucleic acid detection because of their rapid and sensitive response, low cost, operational convenience, and suitability for mass production (Hu et al., 2014; Liu et al., 2011). However, most of these electrochemical biosensors employ only one signaling mechanism, i.e., either "signal-on" or "signal-off" (Hu et al., 2014; Qian et al., 2015). It is no doubt that the simultaneous use of multiple electrochemical labels can provide additional electrochemical information at various redox potentials and robustly detection of specific target molecule (Wei et al., 2014; Xiang et al., 2011; Xiong et al., 2015). Meanwhile, the combination of a biosensor system combined and superimposed dual signal changes as an amplification strategy could be used to analyze target molecule sensitively (Wu et al., 2013; Yang and Lai, 2012). Thus, a truly dual-signaling biosensor that features both "signal-on" and "signal-off" elements was desirable.

Considering the above findings, we first reported a universal electrochemical DNA biosensor based on the spontaneous cascade DNA branch migration strategy and the dual-signaling sensing method for specific and sensitive detection of nucleic acids. A target strand (Ts) competitively hybridized with a ferrocene (Fc)-labeled signal probe (Fc-S1), which was blocked by a protector strand (Ps), after strand displacement to the form Ts/Fc-S1 duplex. A methylene blue (MB)-modified signal probe (MB-S2) was trapped close to the Au electrode surface with the hybridization between the MB-S2 and a thiolated capture probe (Cp). Then, the duplexes (Ts/Fc-S1 and MB-S2/Cp) initiated Holliday junction and formed the Ts/Fc-S1/MB-Sp2/Cp complex. Finally, the obtained four-stranded complex suffered spontaneous DNA branch migration and produced two hybridization products (Fc-S1/Cp and MB-S2/Ts), which resulted in MB molecule departure and Fc molecule conglutination on the Au electrode surface. The detection mechanism of this DNA biosensor involved distance variation between the redox tags and the Au electrode, which was associated with Ts-induced strand displacement reaction and Holliday junction. The proposed biosensor provided a universal and promising method for the selective and sensitive detection of nucleic acids with remarkable advantages, including perfect analytical capability, ease of fabrication, and straightforward operation. Furthermore, dual recognition according to the spontaneous cascade DNA branch migration strategy exhibited an ultrahigh discrimination capability even against single-base mutation.

2. Experimental

2.1. Chemicals and materials

Ethylenediaminetetraacetic acid (EDTA) and Tris (2-carboxyethyl) phosphine hydrochloride (TCEP) were purchased from Sigma-Aldrich Co. (St. Louis, USA). Tris (hydroxymethyl) aminomethane (Tris) and 6-mercapto-1-hexanol (MCH) were supplied by Aladdin Chemistry Co., Ltd. (Shanghai, China). A 20 bp DNA ladder and loading buffer (6 ×) were purchased from TaKaRa Biotechnology Co. Ltd. (Dalian, China). Agarose G-10 was obtained from Biowest, Inc. (Val de Loire, France). Other reagents were of analytical grade and used as received. All solutions were prepared using ultrapure water (Milli-Q 18.2 MΩ cm, Millipore System Inc). HPLC-purified oligonucleotide sequences were purchased from Sangon Biotechnology Inc. (Shanghai, China) and listed in Table S1. The detailed kinetic parameters of the sequences were provided in Table S2.

2.2. Apparatus and measurements

All electrochemical measurements were carried out by using a CHI660D electrochemical workstation (Shanghai CH Instruments Co., China) at room temperature (RT, 25 ± 2 °C). A conventional three-component electrochemical cell comprising a modified Au working electrode (3 mm diameter), a platinum wire auxiliary electrode, and a KCl-saturated Ag/AgCl reference electrode was used. Real-time fluorescence measurements were performed using a Cary Eclipse Fluorescence Spectrophotometer (Agilent, California) with a quartz fluorescence cuvette (45 mm × 12.5 mm × 7.5 mm; path length = 5 mm; inside width = 1 mm). Parameters: Scan time, 60 min; Scanning interval, 1 min; Excitation wavelength, 480 nm; Emission wavelength, 520 nm. An electrophoresis apparatus (DYY-6C, LIUYI, China) was used in the agarose gel electrophoresis experiment. Gel image was recorded by using an imaging system (Bio-Rad Laboratories, USA).

2.3. Electrode pretreatment

The Au electrode was mechanically polished on a microcloth with 0.3 and 0.05 μm alumina powder to obtain a mirror-like surface, followed by successive sonication in ultrapure water, ethanol, and ultrapure water for 5 min each. Then, the electrode was cleaned by immersion in freshly prepared piranha solution (3:1 v/v mixture of 98% H_2SO_4 and 30% H_2O_2) for 10 min (*Caution: Piranha solution dangerously attacks organic matter!*). The Au electrode was further electrochemically pretreated by scanning in H_2SO_4 (0.1 M) between −0.2 and 1.6 V until a stable cyclic voltammogram was obtained, and then the cleaned electrode was rinsed thoroughly and dried with nitrogen gas.

2.4. Preparation of the biosensor

A 2 μM thiol-labeled Cp was first treated with 10 mM TCEP in hybridization buffer (10 mM phosphate buffer, 150 mM NaCl, 70 mM $MgCl_2$, 2.7 mM KCl, pH 7.4) for 1 h at RT to reduce the disulfide bond. MB-S2/Cp conjugation was performed by incubating 1.6 μM Cp with 1.6 μM MB-S2 in the hybridization buffer at 37 °C for 40 min in the dark. The cleaned Au electrode was immersed in a 0.8 μM MB-S2/Cp duplex for 9 h at RT in the dark, and then incubated with 1 mM MCH solution for 1 h at 37 °C to block the uncovered Au electrode surface. The electrode was rinsed thoroughly and ready for the next treatment.

2.5. Electrochemical detection

A 0.8 μM Fc-S1 was first incubated with a 1.2 μM Ps in the hybridization buffer at 37 °C for 40 min to obtain the Fc-S1/Ps duplex. Various concentrations of Ts were further added into the resulting Fc-S1/Ps solution and then incubated at 37 °C for 1 h to displace Ps and form the Ts/Fc-S1 duplex. Subsequently, the obtained mixture solution was dropped on the modified Au electrode. This process was performed in the dark at 37 °C for 80 min and was terminated by repeatedly washing. Finally, square wave

voltammetry (SWV) measurements were performed with a step potential of 4 mV, a frequency of 25 Hz, and an amplitude of 25 mV by scanning the potential from −0.5 V to 0.5 V in working buffer solution (20 mM Tris–HCl, 140 mM NaCl, 5 mM $MgCl_2$, pH 7.4). All analyses were performed in triplicate.

2.6. Real-time fluorescence measurements

Two fluorescence experiments were used to verify the spontaneous cascade DNA branch migration with two pairs of 6-carboxylflouorescein (FAM-) or Dabcyl-modified probes. The FAM- or Dabcyl-modified oligonucleotide sequences were listed in Table S1. In the first experiment, 5′-FAM-labeled S1 (FAM-S1) was premixed with 3′-Dabcyl-labeled Ps (Dabcyl-Ps) at 37 °C for 40 min, and then incubated with Ts. In the second experiment, Ts was first hybridized with the S1/Ps duplex for 40 min at RT to form the Ts/S1 duplex. The obtained mixture was reacted with the FAM-S2/Dabcyl-Cp duplex. Real-time fluorescence of the samples was measured using a fluorescence spectrophotometer for 1 h. The concentrations of each probe and target were 100 nM and 50 nM, respectively.

2.7. Gel electrophoresis

Samples for agarose gel electrophoresis assays were prepared as follows: (1) only Fc-S1 was incubated with Ts; (2) only Fc-S1 was incubated with Ps; (3) Fc-S1 was premixed with Ps for 40 min at 37 °C, and then incubated with Ts. The samples were incubated at 37 °C for 40 min and then subjected to a 3.5% (w/w) agarose gel electrophoresis in 1 × TBE buffer (45 mM Tris–Boric acid, 10 mM EDTA, pH 8.0) at a constant voltage of 100 V for 40 min. The concentration of each sample in agarose gel was 1 μM.

3. Results and discussions

3.1. Mechanism of the proposed biosensor

The detailed principle of this sensing system was illustrated in Scheme 1A. Fc-S1 was first hybridized with Ps to block the orange domain at the 5′ end of Fc-S1 to reduce the background. Green domains of the Fc-S1/Ps duplex and Ts could initiate DNA branch migration to form the Ts/Fc-S1/Ps complex. This complex was inherently unstable, and Ps dissociated from the Ts/Fc-S1/Ps complex, completing the strand displacement reaction and releasing the hybridized product Ts/Fc-S1 duplex. MB-S2 was designed to be partially complementary to the Cp, which allowed the formation of the MB-S2/Cp duplex. The obtained duplexes (Ts/Fc-S1 and MB-S2/Cp) were two primarily double-stranded DNA molecules, and each duplex contained single-stranded overhangs at the 5′ terminal of one strand and at the 3′ terminal of the other. The overhangs with matching color (orange and purple) were complementary to each other. The overhangs of the reactants (Ts/Fc-S1 and MB-S2/Cp) served as “initiation toeholds” to initiate Holliday junction and promote the formation of the Ts/Fc-S1/MB-S2/Cp complex. The four-stranded complex then suffered DNA branch migration through a series of intermediate iso-energetic states. When the toehold-mediated DNA branch migration reached the distal terminus, the “dissociation toeholds” (blue and green) spontaneously fell apart to release two hybridization products

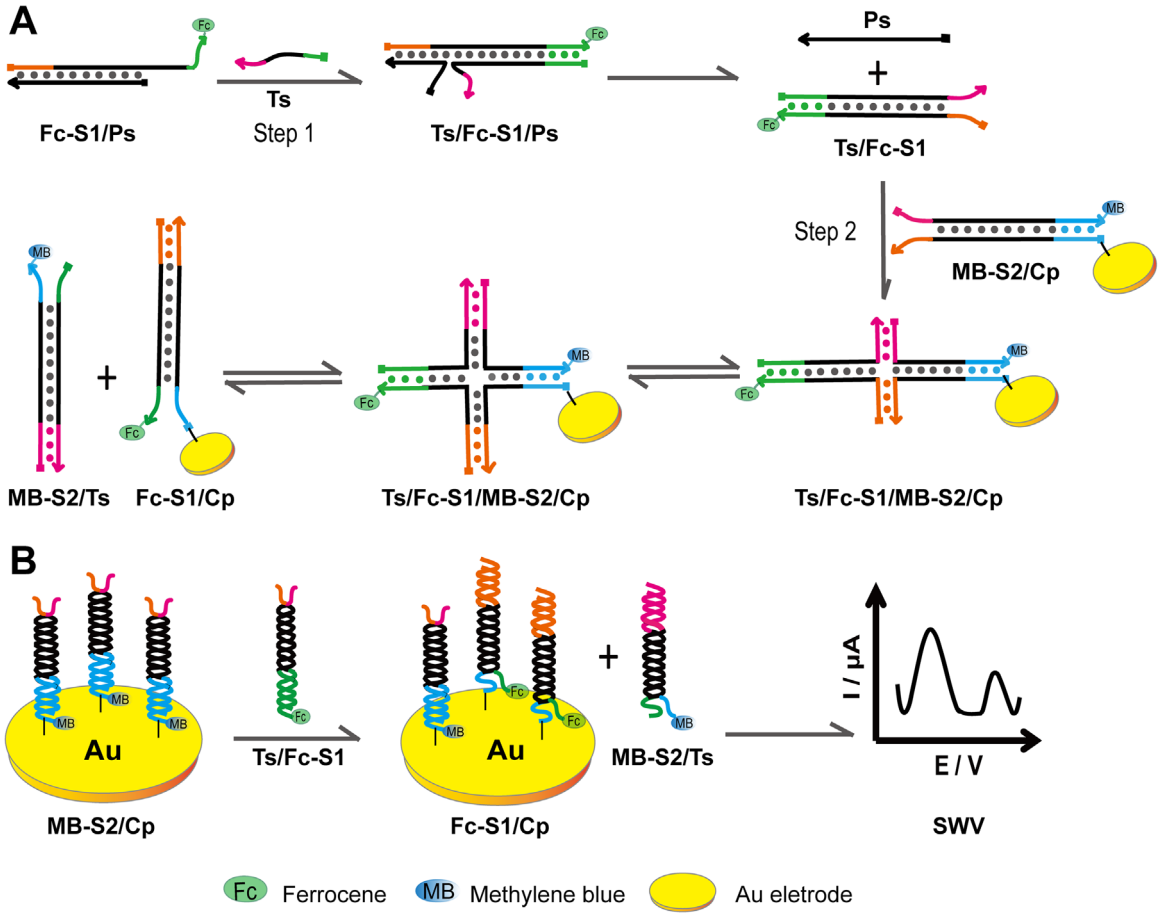

Scheme 1. Illustration of the spontaneous cascade DNA branch migration strategy for target DNA detection. (For interpretation of the references to color in this scheme, the reader is referred to the web version of this article.).

(Fc-S1/Cp and MB-S2/Ts). We designed the MB-S2/Cp duplex rationally to react with the Ts/Fc-S1 duplex with $\Delta G^{\circ} \approx 0$, at which slight thermodynamic changes caused by base mismatch exerted a disproportionately large effect on the hybridization yield. The above cascade DNA branch migration strategy (step1 and step2 in Scheme 1A) provided a dual improved specificity in nucleic acid detection.

MB and Fc were used as the electroactive molecules to produce electrochemical signals in this "signal-on/off" sensing system (Scheme 1B). The MB-S2/Cp duplex was first self-assembled on the Au electrode surface through Au–S bond, and then kept upright because of the immobilized MCH. Hence, the MB molecule was confined near the electrode surface, producing an intense current signal. When challenged with the Ts/Fc-S1 duplex, MB-S2 dissociated from the MB-S2/Cp duplex into the solution, and Fc-S1 attached to Cp. These changes led to the decrease of the redox current of MB (I_{MB}), accompanied by the increase of that of Fc (I_{Fc}). Analysis of Ts relied on the simultaneous monitoring of MB signal suppression and Fc signal enhancement. The value of $\Delta I_{Fc}+|\Delta I_{MB}|$ was used to quantify target concentration and thus amplify the signal. These designs significantly improved the selectivity and sensitivity of nucleic acid detection.

3.2. Characterization of the sensing system

To verify the concept of the cascade branch migration strategy, the *mecA* gene in methicillin-resistant *Staphylococcus aureus* was selected as the model target to test whether or not our design functions as intended. We first carried out two experiments to verify the spontaneous cascade DNA branch migration using two pairs of FAM- or Dabcyl-modified probes (Fig. 1A). Clearly, no signal was obtained when Ts was omitted from the reaction (curve a in Fig. 1A) because Dabcyl can quench FAM fluorescence upon the hybridization between FAM-S1 and Dabcyl-Ps. By contrast, the fluorescence intensity gradually increased when the FAM-S1/Dabcyl-Ps duplex was incubated with Ts (curve b in Fig. 1A), implying that the strand displacement reaction was successfully initiated. This process was further confirmed by gel electrophoresis (Fig. 1B). The gel electrophoresis of the strand displacement reaction products showed that a band (lane 3) lying in the position of the Ts/Fc-S1 duplex (lane 1). This suggested that the Ts displaced the Ps successfully. The significant fluorescence variation upon the hybridization between the Ts/S1 and FAM-S2/Dabcyl-Cp duplexs reflected that the toehold-mediated Holliday junction spontaneously occurred (curve c in Fig. 1A). Therefore, the above results demonstrated the successful design of the sensing system.

The stepwise fabrication of this biosensor was monitored using cyclic voltammetry (CV) and electrochemical impedance spectroscopy (EIS). CV measurements were employed to characterize the changes in electrochemical properties during the modification process. As exhibited in Fig. 1C, a couple of strong redox peaks of MB was observed at −0.28 and −0.29 V in the potential window

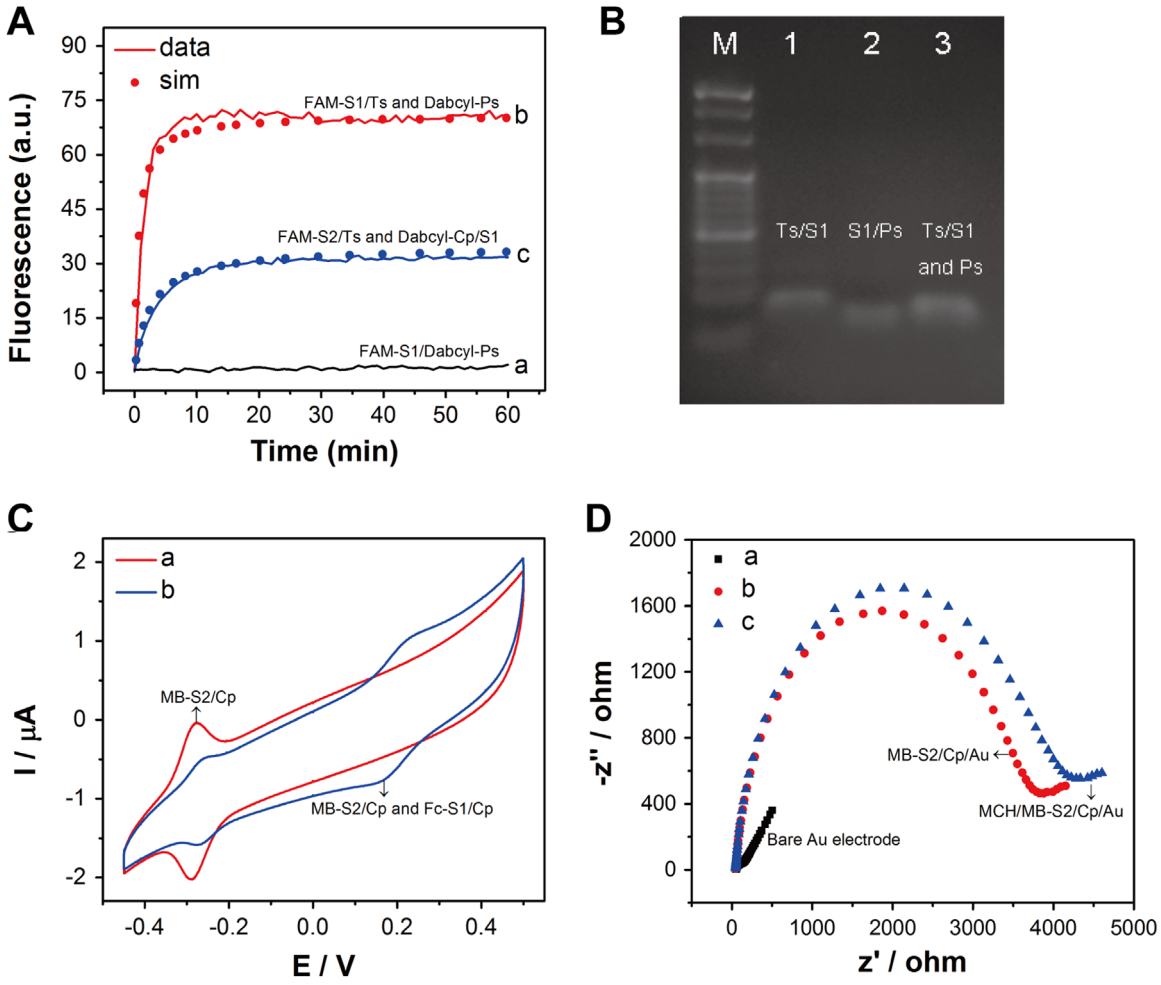

Fig. 1. Characterization of the sensing system. (A) Fluorescence intensity of: (a) FAM-S1/Dabcyl-Ps; (b) FAM-S1/Dabcyl-Ps+Ts; and (c) FAM-S2/Dabcyl-Cp+S1/Ps in the presence of Ts. Dotted lines showed simulation results (sim) calculated with the second order reaction. (B) Agarose gel electrophoresis of: (1) Ts/Fc-S1; (2) Fc-S1/Ps; and (3) Fc-S1/Ps+Ts. (C) CVs of: (a) MB-S2/Cp/Au; and (b) MB-S2/Cp/Au+Fc-S1/Ps in the presence of Ts. (D) EIS of: (a) bare Au electrode; (b) MB-S2/Cp/Au; and (c) MCH/MB-S2/Cp/Au.

(curve a), which indicated that the MB-S2/Cp duplex was immobilized on the surface of the Au electrode. When hybridized with the Ts/Fc-S1 duplex, the redox current of MB declined whereas that of Fc dramatically increased (curve b). Such changes implied that a large amount of MB molecules moved away from the electrode surface, and that a large amount of Fc molecules were loaded onto the Au electrode. The CV results in Scheme 1A demonstrated the success of DNA branch migration in double-stranded DNA according to step2. EIS was also employed to characterize the fabrication of this sensing system (Fig. 1D). The bare Au electrode showed a very small semicircle domain (curve a), which demonstrated the excellent electron transfer ability of the Au electrode. The impedance increased after immobilization of the MB-S2/Cp duplex (curve b), suggesting that the MB-S2/Cp duplex was successfully combined on the electrode surface through Au–S bond. The semicircle further increased after MCH immobilized on the Au electrode (curve c), implying that the immobilized MCH inhibited electron transport to the electrode surface with non-conductive properties. Similarly, these observations showed the success of the stepwise modification.

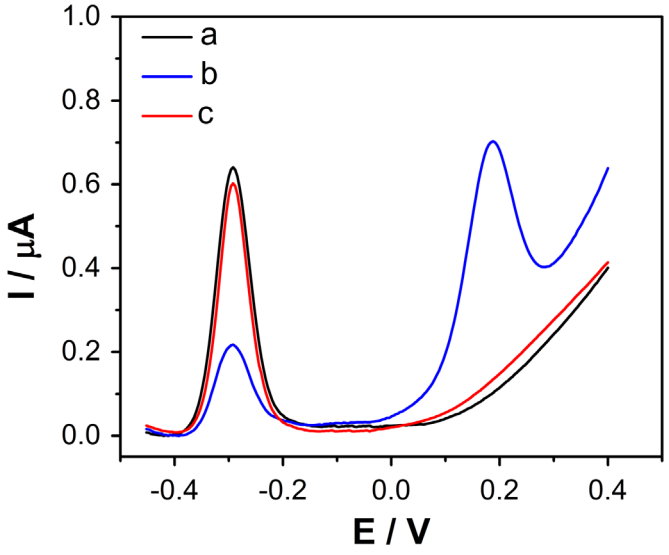

Fig. 2. Feasibility of the dual-signaling electrochemical biosensor. SWVs of: (a) MB-S2/Cp/Au; (b) MB-S2/Cp/Au+Fc-S1/Ps in the presence of Ts; and (c) MB-S2/Cp/Au+Fc-S1/Ps in the absence of Ts (blank).

3.3. Feasibility of the dual-signaling electrochemical biosensor

The SWV responses of the different modified electrodes were measured (Fig. 2) to demonstrate the feasibility of the proposed "signal-on/off" biosensor for target detection. After the immobilization of the MB-S2/Cp duplex, only a well-defined current peak of MB at approximately −0.29 V was measured because the MB molecule transferred the electrode efficiently (curve a). When the modified Au electrode was further incubated in Fc-S1/Ps

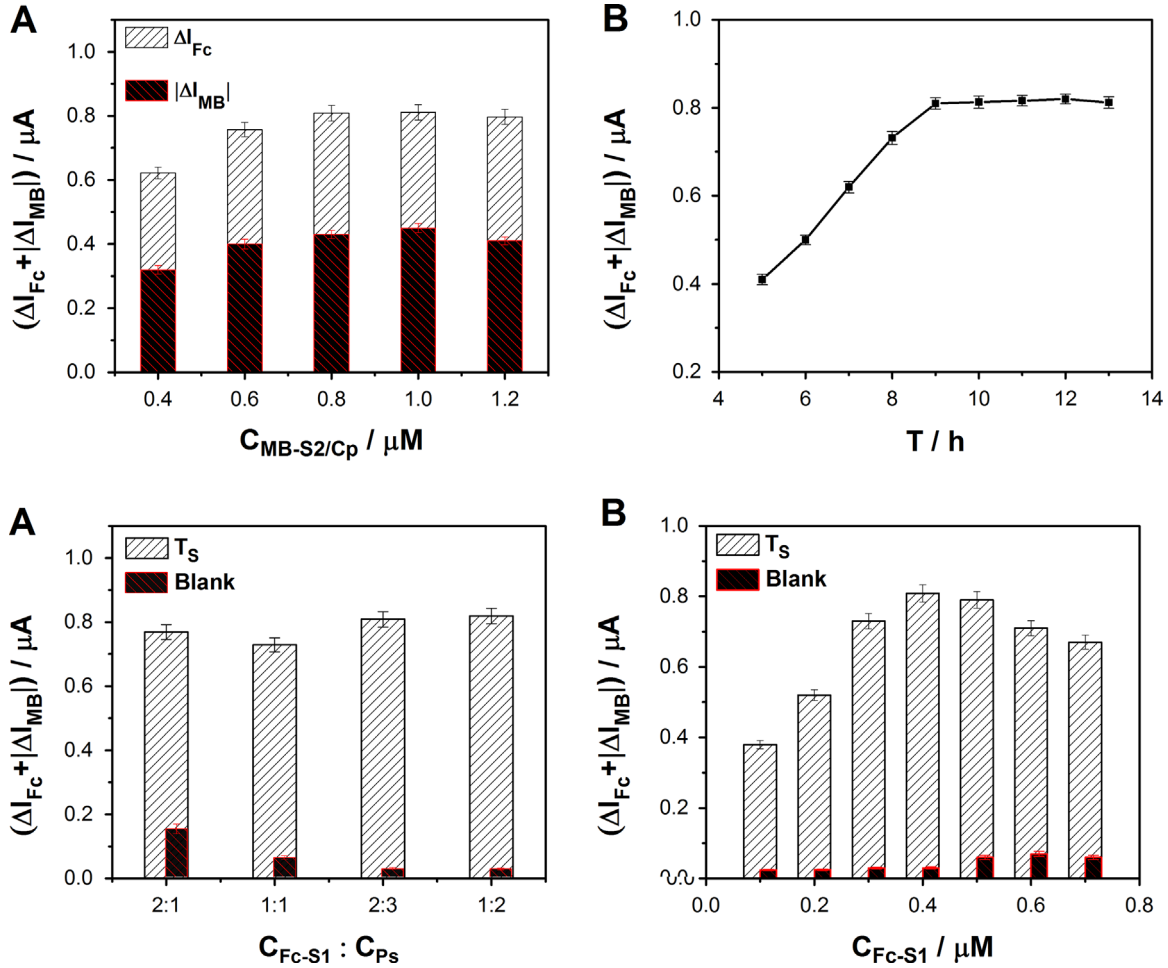

Fig. 3. Optimization of the experimental conditions. Effects of (A) MB-S2/Cp duplex concentration; (B) self-assembly time; (C) concentration ration of Fc-S1 versus Ps; (D) Fc-S1 concentration on the electrochemical response in this sensing system. The used concentrations were 0.4, 0.6, 0.8, 1.0, 1.2 μM, respectively. When one parameter changed, the others kept on their optimal conditions. The target DNA concentration was 2 nM. Error bars represented standard deviations of the measurements ($n=3$).

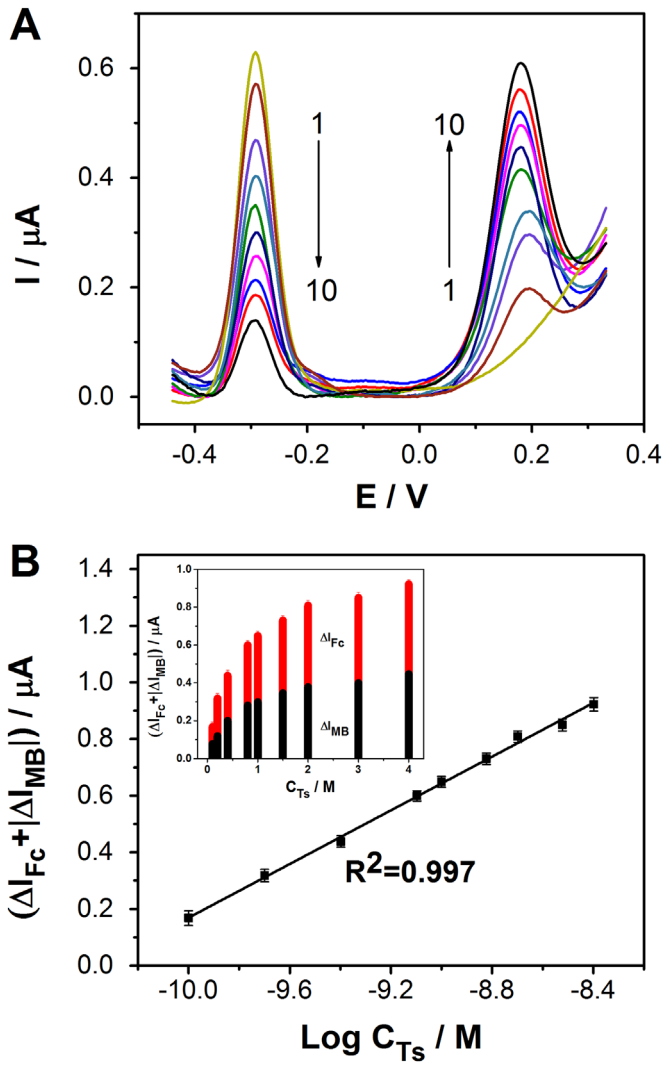

Fig. 4. Analytical performance of the DNA biosensor. (A) SWVs of the "signal-on/off" system with the increasing concentrations of Ts (from 1 to 10: 0, 0.1, 0.2, 0.4, 0.8, 1, 1.5, 2, 3, and 4 nM, respectively). (B) Calibration curve of $\Delta I_{Fc}+|\Delta I_{MB}|$ versus the logarithm of Ts concentrations. Inset: the relationship between the $\Delta I_{Fc}+|\Delta I_{MB}|$ and the concentrations of Ts. Error bars represented standard deviations of the measurements ($n=3$).

solution in the presence of Ts, the MB response was significantly suppressed, whereas the Fc response increased (curve b). As a result, the observed variation in the MB and Fc currents originated from the MB-S2 dissociation and the Fc-S1 collection during the DNA branch migration. Moreover, the redox currents of MB and Fc slightly changed in the absence of Ts because the Fc-S1/Ps duplex was unable to react with the MB-S2/Cp duplex without the target (curve c). The above results suggested that the Fc-S1 acted as a conventional "signal-on" probe in this sensing system, whereas the MB-S2 acted as a "signal-on" probe. In conclusion, this developed electrochemical biosensor produced a readily measured current variation that could be related to the presence and concentration of Ts.

3.4. Optimization of the experimental conditions

The corresponding experimental conditions were selectively optimized to achieve the perfect sensing performance. The immobilization order of Cp and MB-S2 probes was firstly optimized. As shown in the Fig. S1, curve a was obtained when Cp was immobilized on the gold surface at the first and then hybridized with MB-S2, curve b was obtained when Cp hybridized with S2 at the first. The electrochemical signal of curve a was much less than that of curve b which suggesting the second method was better for this electrochemical biosensor. Previous studies indicated that the hybridization efficiency increases with increasing probe density, but signal suppression increases with increasing probe density. Hence, the concentration and the incubation time of the MB-S2/Cp duplex should be optimized. As shown in Fig. 3A, $\Delta I_{Fc}+|\Delta I_{MB}|$ increased with MB-S2/Cp concentration from 0.4 μM to 0.8 μM. The concentration further increased with a slight decrease in signal variation. The dependence of $\Delta I_{Fc}+|\Delta I_{MB}|$ on the immobilization time of MB-S2/Cp was studied in the range of 5–13 h (Fig. 3B). The results showed that the current variation gradually increased with prolonged time and then stabilized after 9 h. Therefore, 0.8 μM and 9 h were selected as the optimal concentration and immobilization time of the MB-S2/Cp duplex, respectively. The concentration ration of Fc-S1 versus Ps and the concentration of Fc-S1 were also optimized to maximize the signal-to-noise ratio and the detection sensitivity. As illustrated in Fig. 3C and D, the no color filling pillar represented the current variation obtained in the presence of Ts. The color filling pillar represented the background signal. Results indicated that the optimal concentration ration of Fc-S1 versus Ps and the optimal concentration of Fc-S1 were 2:3 and 0.4 μM, respectively. Basing from the optimized conditions mentioned above, we also investigated the time and temperature of the Holliday junction (Fig. S2). Results suggested that an optimum time of 80 min and a temperature of 37 °C were the ideal reaction conditions for the following experiments.

3.5. Analytical performance of the DNA biosensor

Under the optimal experimental conditions, the sensitivity of the fabricated biosensor was determined using a series of Ts concentrations. As shown in Fig. 4A, the MB current decreased and the Fc current increased with increasing concentrations of Ts (curves 1–10). The dependence of the variation of MB current or Fc current on the logarithm of Ts concentration was analyzed on the basis of the individual MB or Fc signals (Fig. S2A). Both of the resulting calibration curves exhibited a linear relationship in the range of −10 to −8.4, and the detection limits were 114 and 161 pM ($S/N=3$) corresponding to the MB and Fc signals, respectively. To amplify the electrochemical response, $\Delta I_{Fc}+|\Delta I_{MB}|$ was used as the response signal to determine quantitatively the concentration of Ts (insert in Fig. 4B). The value of $\Delta I_{Fc}+|\Delta I_{MB}|$ was linear with the logarithm of Ts concentration (Figs. 4B and S3B). The regression equation was expressed as $\Delta I_{Fc}+|\Delta I_{MB}|$ (μA)= 4.899+0.473 log C (M) with a coefficient of determination (R^2) of 0.997, where C is the concentration of Ts ($n=3$). The detection limit was estimated at 85 pM ($S/N=3$). Obviously, the proposed method in this study showed good performance in terms of analytical range and detection limit.

3.6. Specificity of this sensing system

The specificity of the fabricated spontaneous cascade DNA branch migration strategy and the dependence of the differentiating ability on the mutant type were also evaluated using Ts, a series of mutant target (Mt) molecules (Table S1) and blank. These base changes were distributed at the middle position along the testing region and included insertions, deletions and mismatch. As shown in Fig. 5, various mutant sequences all produced slight current changes, which were considerably lower than the current variation in the presence of Ts. The ΔG° of hybridization changed with the types of mutation, which resulted in different discrimination capacities (insert in Fig. 5). The discrimination factor

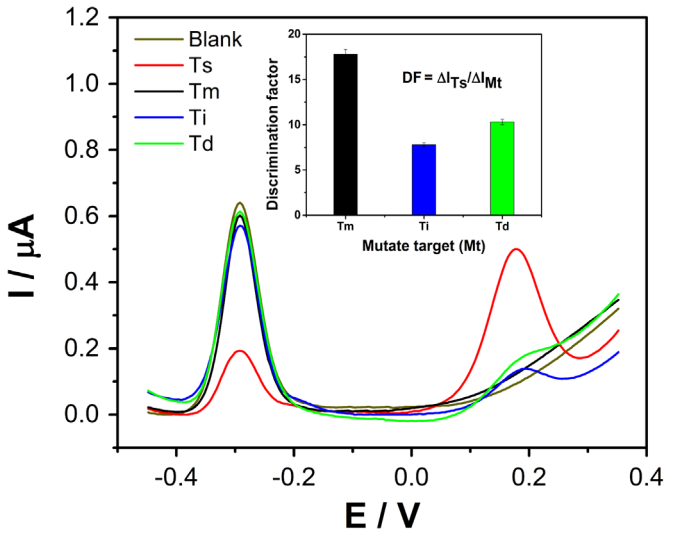

Fig. 5. Specificity of this sensing system. SWVs of: blank; (Ts) complementary target; (Tm) mismatch target; (Ti) insert target; and (Td) delete target. Inset: the dependence of the discrimination factors ($DF=\Delta I_{Ts}/\Delta I_{Mt}$) on different mutate types. The DNA concentration was 2 nM. Error bars represented standard deviations of the measurements ($n=3$).

($DF=\Delta I_{Ts}/\Delta I_{Mt}$) quantified the specificity of this sensing system as the ratio of the current change generated by equal concentrations of Ts and Mt molecules. The highest DF was obtained with the mismatch sequence and DFs of the mutant sequences ranged from 7.8 to 17.9, with a median of 12. These above results clearly demonstrated that the present sensing system based on the cascade recognition strategy had a high sequence specificity to distinguish Mt.

4. Conclusion

In short, using the spontaneous cascade DNA branch migration reaction and dual-signaling sensing strategy, we first introduced a universal electrochemical biosensor for the highly specific and sensitive detection of nucleic acids. With the aid of the truly dual-signaling amplification method and the simple signal transduction manner, the proposed electrochemical biosensor exhibited remarkable advantages including perfect analytical capability, ease of fabrication and straightforward operation. The spontaneous cascade DNA branch migration strategy also exhibited an apparent improved specificity and an ultrahigh discrimination capability even against single-base mutation because of dual recognition. Importantly, this electrochemical DNA biosensor could be conveniently applied to other nucleic acids simply by altering the corresponding DNA sequences. Therefore, the proposed DNA biosensor has a great potential for further applications in biomedical research, food safety, early clinical diagnosis, and environmental monitoring.

Acknowledgments

This work was supported by the National Natural Science Foundation of China (No. 81171415).

Appendix A. Supplementary material

Supplementary data associated with this article can be found in the online version at http://dx.doi.org/10.1016/j.bios.2015.11.071.

References

Agarwal, K., Kaul, R., Garg, M., Shajahan, A., Jha, S.K., Sampathkumar, S.-G., 2013. J. Am. Chem. Soc. 135, 14189–14197.
Chen, A., Gui, G., Zhuo, Y., Chai, Y., Xiang, Y., Yuan, R., 2015. Anal. Chem. 87, 6328–6334.
Chen, J., Zhang, J., Guo, Y., Li, J., Fu, F., Yang, H.-H., Chen, G., 2011. Chem. Commun. 47, 8004–8006.
Chen, S.X., Zhang, D.Y., Seelig, G., 2013. Nat. Chem. 5, 782–789.
Collins, F.S., Green, E.D., Guttmacher, A.E., Guyer, M.S., 2003. Nature 422, 835–847.
Farjami, E., Clima, L., Gothelf, K., Ferapontova, E.E., 2011. Anal. Chem. 83, 1594–1602.
Genot, A.J., Zhang, D.Y., Bath, J., Turberfield, A.J., 2011. J. Am. Chem. Soc. 133, 2177–2182.
Gomez, A., Miller, N.S., Smolina, I., 2014. Anal. Chem. 86, 11992–11998.
Hu, Y., Xu, X., Liu, Q., Wang, L., Lin, Z., Chen, G., 2014. Anal. Chem. 86, 8785–8790.
Ito, T., Hosokawa, K., Maeda, M., 2007. Biosens. Bioelectron. 22, 1816–1819.
Krainer, G., Hartmann, A., Schlierf, M., 2015. Nano Lett. 15, 5826–5829.
Li, B., Ellington, A.D., Chen, X., 2011. Nucleic Acids Res. 39, e110-e110.
Li, C., Li, Y., Xu, X., Wang, X., Chen, Y., Yang, X., Liu, F., Li, N., 2014. Biosens. Bioelectron. 60, 57–63.
Liu, Z., Zhang, W., Zhu, S., Zhang, L., Hu, L., Parveen, S., Xu, G., 2011. Biosens. Bioelectron. 29, 215–218.
Panyutin, I.G., Hsieh, P., 1993. J. Mol. Biol. 230, 413–424.
Qian, L., Winfree, E., Bruck, J., 2011. Nature 475, 368–372.
Qian, Y., Tang, D., Du, L., Zhang, Y., Zhang, L., Gao, F., 2015. Biosens. Bioelectron. 64, 177–181.
Ren, K., Wu, J., Yan, F., Zhang, Y., Ju, H., 2015. Biosens. Bioelectron. 66, 345–349.
Sauna, Z.E., Kimchi-Sarfaty, C., 2011. Nat. Rev. Genet. 12, 683–691.
Wang, F., Lu, C.-H., Willner, I., 2014. Chem. Rev. 114, 2881–2941.
Wang, J.S., Zhang, D.Y., 2015. Nat. Chem. 7, 545–553.
Wei, T., Chen, Y., Tu, W., Lan, Y., Dai, Z., 2014. Chem. Commun. 50, 9357–9360.
Wu, L., Zhang, X., Liu, W., Xiong, E., Chen, J., 2013. Anal. Chem. 85, 8397–8402.
Xiang, Y., Qian, X., Chen, Y., Zhang, Y., Chai, Y., Yuan, R., 2011. Chem. Commun. 47, 2080–2082.
Xiong, E., Zhang, X., Liu, Y., Zhou, J., Yu, P., Li, X., Chen, J., 2015. Anal. Chem. 87, 7291–7296.
Yang, W., Lai, R.Y., 2012. Chem. Commun. 48, 8703–8705.
Zhang, D.Y., 2010. J .Am. Chem. Soc. 133, 1077–1086.
Zhang, D.Y., Chen, S.X., Yin, P., 2012. Nat. Chem. 4, 208–214.
Zhang, D.Y., Seelig, G., 2011. Nat. Chem. 3, 103–113.
Zhang, D.Y., Winfree, E., 2010. Nucleic Acids Res. 38, 4182–4197.
Zhu, J., Zhang, L., Li, T., Dong, S., Wang, E., 2013. Adv. Mater. 25, 2440–2444.